Marangoni forces created by surface plasmon decay

R. H. Farahi, A. Passian, T. L. Ferrell, and T. Thundat

Oak Ridge National Laboratory, Oak Ridge, Tennessee 37831

Received September 15, 2004

We present optical microfluidic manipulation of silicone oil and glycerol via surface tension driven forces sustained by surface plasmon deexcitation energy. The phonon energy associated with the decaying optically excited surface plasmons in a thin gold foil creates thermal gradients capable of actuating fluid flows. Spectral dependence of the plasmon decay length and control of optical beam characteristics are shown to provide a means for further manipulation. © 2005 Optical Society of America

OCIS codes: 240.6680, 120.6810.

Systems that are able to manipulate microfluids can vary greatly with their architecture and flow actuation schemes. In such systems fluids are rendered on an open surface or encapsulated inside a microchannel or a small volume. Open surface fluid regulation may be accomplished with surface tension modulation in which the thermocapillary forces between a liquid droplet and a solid surface combined with local variations in surface tension may set the liquid in motion. This surface tension driven flow is known as the Marangoni effect.[1–6] A surface tension gradient can be created by several approaches, including composition, chemical,[7,8] electrochemical,[9] thermal,[10,11] photochemical,[12] and optical.[13] A dynamically applied surface tension gradient at one or more specified locations is best achieved with the last four of these approaches. Often spatially confined thermal gradients have been produced and controlled with resistive heating elements. We recently reported a thin film variation of such a system in which a mesh of thin gold (Au) wires and the consequent thermal pattern facilitated the fluid actuation.[14] In this Letter we report on an optical approach of providing the required temperature gradient that relies on the collective electronic excitation[15] in a thin solid foil on a dielectric substrate. We demonstrated how optical excitation of surface plasmons,[16] typically realized in the Kretschmann configuration,[17] subsequently generates sufficient heat in metal film to alter the surface energy of the liquid and thus induce motion via Marangoni forces. The complex dielectric function of the foil material and the surface roughness are responsible for the decay of surface plasmons into phonons. Surface plasmons are excited when the dispersion relation of the incident radiation striking a thin metal foil matches that of the surface plasmon at some point, and consequently the surface plasmon energy decays into radiative, acoustic, and thermal energy. Here we present Marangoni flows of silicone oil (SO) and glycerol facilitated by a localized heat source created by the deexcitation of surface plasmons.

Surface plasmons are optically excited on a 34 nm thick Au film mounted in the Kretschmann configuration shown in Fig. 1. The incident light is an Ar^+ laser ($\lambda = 514$ nm) that is p polarized and collimated to a 100-μm-diameter spot on the Au surface. Surface plasmon excitation occurs as a result of the absorption of incoming photons, which is manifested by the observation of a minimum in the reflected spectrum. Depending on the extent of the surface roughness, a spot of visible scattered radiation appears on the film surface, indicating the radiative coupling of the plasmons. It should be noted that the incident light was slightly decollimated to achieve the tightest spot size, causing a small variation of angles in the incident beam. The angle of incident light was tuned to maximize coupling of the incident light at the Au–air interface (peak absorption). For the parameters of our experiment this surface plasmon angle (θ_{sp}) was 52°. We deposited small droplets with different indices of refraction (n), surface tension (σ), dynamic viscosity (ν), and contact angle (θ_c) on the Au surface by bringing a lightly wetted curved wire (gauge 42) near the surface until a meniscus formed between the surface

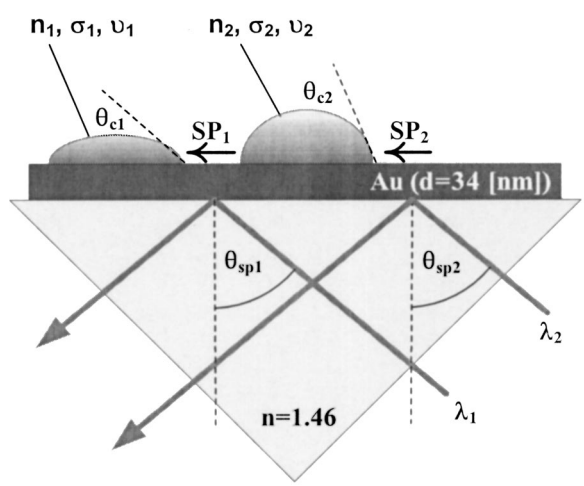

Fig. 1. Schematic of the Kretschmann configuration including the droplets. A right-angle quartz ($n = 1.46$) prism, is Au coated by vacuum evaporation to form a 34-nm thin film. Several droplets (index of refraction n_i, surface tension σ_i, viscosity ν_i, $i = 1, 2, \ldots$) are disposed on the surface of the Au, where a temperature gradient prevails because of the decay of surface plasmons. Photons of wavelength λ excites the plasmons at an angle θ_{sp} determined for the free Au surface. The contact angles of the droplets were measured to estimate their curvature.

0146-9592/05/060616-3/$15.00 © 2005 Optical Society of America

and the wire. When the wire was removed, a droplet as small as 30 μm in diameter remained on the surface. With this straightforward technique we show in Figs. 2(a)–2(e) that the applied SO droplet ($n=1.405, \sigma=0.021$ N/m, $\nu=0.095$ Pa s) was 150 μm in width, 420 μm in length, and 20 μm in height. As shown in Figs. 2(f)–2(l), the applied glycerol droplet ($n=1.451, \sigma=0.063$ N/m, $\nu=1.485$ Pa s) was approximately 240 μm in diameter and 50 μm in height. The laser power required to create a sufficient thermal gradient for the transport of the droplets across the surface was measured with a calibrated powermeter. In the absence of the liquid, surface plasmon coupling was measured to be ~92%, taking into account a 4% loss through the quartz crystal. For SO in Figs. 2(a)–2(e) and glycerol in Figs. 2(f)–2(l), the power was 45 and 72 mW, respectively. As expected, the disparity in power was due to the difference in mass, σ, and ν of the droplets. The surface plasmon excitation region (the spot) is positioned near the droplet as shown in Figs. 2(a) and 2(f). As the spot is steered toward the droplet several events occur. The form of the droplet begins to undergo a disturbance when the physical boundary of the spot is approximately 30 μm away in the direction of surface plasmon propagation, indicating that a thermal gradient extends beyond the region of plasmon coupling, shown in Fig. 2(f). We note that the surface plasmon decay length (e-folding) for our working wavelength ($\lambda=514$ nm) and metal[18] ($\epsilon=-3.9+2.7i$) is approximately 0.52 μm.

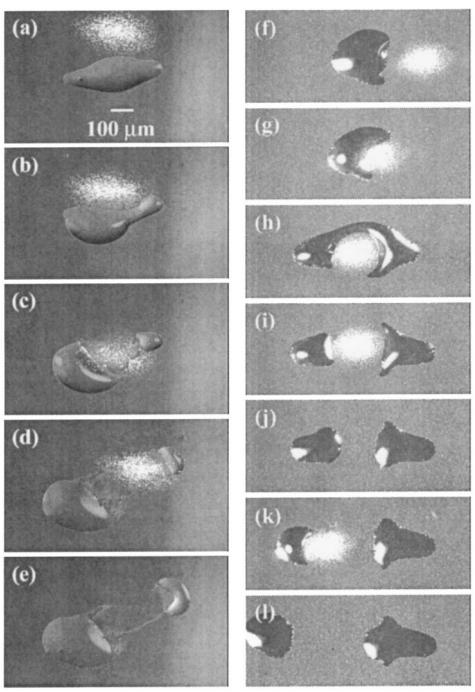

Fig. 2. Demonstration of surface tension driven manipulation by surface plasmons of (a)–(e) a silicone droplet and (f)–(l) a glycerol droplet. The silicone droplet contact angle is $\theta_c=10°$, whereas that of the glycerol is 50°. The scale bar in (a) represents the dimensions in all the displayed images. The incident beam, generating the excitation region (bright spot) seen above the droplet in (a) facilitates the droplet actuation. The beam is blocked in (c), (j), and (l) to better show the resulting state of the liquid droplets. For viewing purposes the silicone droplet was illuminated from the bottom and the glycerol droplet was illuminated from the top. The topside illumination highlighted the surface roughness of the Au film. The droplets are distorted in shape because of the geometric asymmetries in the thermal gradient.

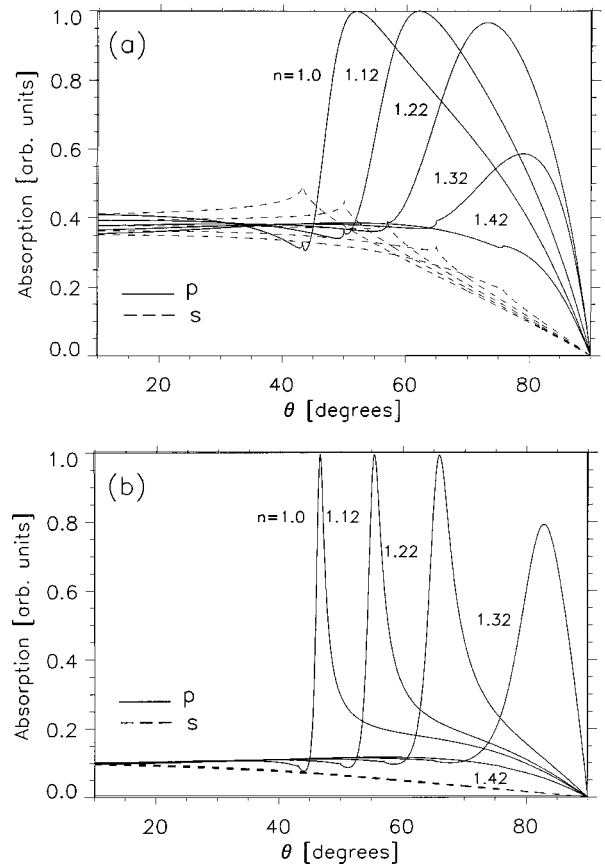

Fig. 3. Relative modification of the surface plasmon excitation as a result of the variation of the dielectric function of the liquid in the Kretschmann configuration. The simulation was made for (a) 34 nm thick Au film at the $\lambda=514$ nm line of an Ar^+ laser and (b) 54 nm thick Au film at the $\lambda=632.8$ nm line of a He–Ne laser for both p and s polarizations. As can be seen, apart from an angular shift, the resonance conditions deteriorate drastically for the chosen film for n as low as 1.4.

For SO in Fig. 2(b), and glycerol in Fig. 2(g), part of the droplet increases in temperature, decreases in viscosity, reduces surface tension, and recedes from the oncoming thermal gradient. As the laser beam begins to travel underneath the droplet, the coupling efficiency drops because the changes in the refractive index over the Au film alter the resonance conditions. This is shown in Fig. 3, which compares the effect of the presence of the droplet on the plasmon excitation for an index of refraction in the range $1.0 \leqslant n \leqslant 1.42$ at two wavelengths. Also, as can be seen from Fig. 3, there is still enough plasmon excitation to maintain a thermal gradient underneath the droplets, albeit a smaller one (<40% at $n=1.42$). At such levels the s polarization will have the same thermal effect for the 514 nm line in Fig. 3(a), whereas negligible absorp-

tion is seen in the case of 632.8 nm in Fig. 3(b).

Measuring the intensity of reflected light shows that the coupling efficiency of the SO and the glycerol droplets was reduced to approximately 67% and 73%, respectively. Note that in Fig. 2(h) the glycerol droplet starts to surround the heated region because it is too large to be entirely transported by the localized thermal gradient and its surface tension is higher. The plasmon coupling efficiency of 92% eventually is restored as the droplet flows out of the spot region without wetting the surface. Once the larger droplet has been cut into two smaller droplets, microfluid transport by surface plasmons is demonstrated in Figs. 2(c)–2(e) for SO and in Figs. 2(i)–2(l) for glycerol.

In conclusion, we have demonstrated all-optical manipulation of droplets on metal surfaces. Excitation and modulation of surface plasmons for the particular purpose presented here is a new concept that offers several possibilities to be explored. Materials with dielectric functions that do not exhibit absorption at the plasmon excitation frequencies, such as transparent silicone oil, are readily manipulated based on the results presented. Absorptive materials can be manipulated by use of plasmon excitation in spectral regions away from those of the material. Although limited absorption may not hinder actuation, this matter requires further investigation and is currently under study. Proper selection of foil and substrate material and patterning the foil can further help optimize the performance. The presented effect opens new possibilities in optical systems by which the droplet can be integrated as an optical component.

This work was supported by the DOE Office of Biological and Environmental Research (OBER) and by the Department of Energy—Basic Energy Sciences (DOE-BES). Oak Ridge National Laboratory, Oak Ridge, Tennessee 37831-6123, is managed by UT-Battelle, LLC for the Department of Energy under contract number DE-AC05-0096OR22725. R. H. Farahi's e-mail address is farahirh@ornl.gov.

References

1. C. G. M. Marangoni, Ann. Phys. Chem. (Poggendorf) **143**, 337 (1871).
2. L. E. Scriven and C. V. Sternling, Nature (London) **187**, 186 (1960).
3. J. Thomson, Philos. Mag. Ser. **10**, 330 (1855).
4. P. Dell'Aversana and G. P. Neitzel, Phys. Today **51**(1), 38 (1998).
5. R. Monti, R. Savino, and G. Alterio, Acta Astronaut. **51**, 789 (2002).
6. P. Dell'Aversana, V. Tontodonato, and L. Carotenuto, Phys. Fluids **9**, 2475 (1998).
7. M. K. Chaudhury and G. M. Whitesides, Science **256**, 1539 (1992).
8. S. Daniels, M. K. Chaudhury, and J. C. Chen, Science **291**, 633 (2001).
9. B. S. Gallardo, V. K. Gupta, F. D. Eagerton, L. I. Jong, V. S. Craig, R. R. Shah, and N. L. Abbott, Science **283**, 57 (1999).
10. R. Savino, R. Monti, and G. Alterio, Phys. Fluids **13**, 1513 (2001).
11. A. A. Darhuber, J. P. Valentino, J. M. Davis, S. M. Troian, and S. Wagner, Appl. Phys. Lett. **82**, 657 (2003).
12. K. Ichimura, S. Oh, and M. Nakagawa, Science **288**, 1624 (2000).
13. N. Garnier, R. O. Grigoriev, and M. F. Schatz, Phys. Rev. Lett. **91**, 054501 (2003).
14. R. H. Farahi, A. Passian, T. L. Ferrell, and T. Thundat, Appl. Phys. Lett. **85**, 4237 (2004).
15. R. H. Ritchie, Phys. Rev. **106**, 874 (1957).
16. T. L. Ferrell, T. A. Callcott, and R. J. Warmack, Am. Sci. **73**, 344 (1985).
17. E. Kretschmann, Z. Phys. **241**, 313 (1971).
18. E. D. Palik, *Handbook of Optical Constants of Solids* (Academic, Orlando, Fla., 1985).